

LS-79
January 6, 1987

BUILDING-SOIL VIBRATION COUPLING

by

J. A. Jendrzejczyk, R. K. Smith

Materials and Components Technology Division

BUILDING-SOIL VIBRATION COUPLING

by

J. A. Jendrzejczyk and R. K. Smith

Materials and Components Technology Division

1.0 OBJECTIVES

Develop an understanding of building-soil coupling

Verify instrumentation sensitivity

2.0 DATES AND TIMES

November 6, 1986; ~ 1:00 PM to 4:30 PM

November 7, 1986; ~ 9:30 AM to 11:30 AM

3.0 LOCATION

Basement service level of Building 335 and front lawn between building and road (see Fig. 1, Measurement Locations)

4.0 EXCITATION SOURCE

A Worthington 5" x 5", 7-1/2 HP air compressor was used as the excitation source. The compressor is of the reciprocating type with a 7" motor drive sleeve. A 25" sleeve is mounted to the compressor. With the factor 0.269 for speed reduction and a motor speed of 1750 RPM an excitation force with a frequency of 7.85 Hz was generated. A smaller force at ~ 15.7 Hz is associated with operation of the valve assembly of the compressor. The compressor is mounted on a concrete pad which is isolated from the building floor by means of a 3/4" tar expansion joint.

5.0 INSTRUMENTATION

PCB Accelerometer, Model No. 393C. For soil measurements the accelerometer was mounted vertically using a #10-32 stud on a 1-1/8" x 22" SST rod driven ~ 18" into the ground. For measuring the floor and pad motion, 3" x 3" x 1/4" aluminum plates were epoxied to the concrete surfaces and the accelerometer was attached to the plates with #10-32 studs.

PCB Model No. 480A10 Battery Operated Dual Integrating Amplifier. The amplifier provides power and also double integration of the acceleration signal to obtain displacements.

6.0 MEASUREMENTS

Ground motion (acceleration and displacement) was measured at the four measurement locations identified in Fig. 1. Due to the position of the road, it was necessary to locate the 93' and 135' measurement stations on diagonals.

7.0 DATA

- a) Accelerations and displacements were measured at all measurement locations with and without the air compressor running. This allows for a comparison of the response due to compressor excitation with the ambient noise level.
- b) Data are presented in terms of mean-square acceleration and displacement versus frequency on linear coordinates to facilitate calculation of amplitudes at various frequencies. Log-log plots of rms acceleration and displacement are also plotted to allow for comparison with other data and for easy identification of frequencies. Calibration verification of the 5451C FFT (Fast Fourier Transform) Analyzer is given in Fig. 2. Displacement data are given in Figs. 3-8 and accelerometer data are given in Figs. 9-14.

8.0 DISCUSSION

The rms displacement noise levels corresponding to the various measurement locations are given in Table 1. The ambient displacement noise level (compressor off) remains fairly constant, while a decrease in displacement amplitude with distance is observed in the compressor-on data. Ambient noise level (compressor off) displacement power spectra are shown in Fig. 3. A frequency peak at approximately 12 Hz is observed in and near the building, decreasing in amplitude with increasing distance from the building which indicates the excitation source is within the building. No attempt was made to locate it. The area under the power spectrum response plots is shown in Fig. 4. Vertical amplitude is proportional to displacement squared. From these plots, amplitude contributions at various frequencies can easily be calculated.

To compare measured data with available published data the linear displacement spectra were plotted in log-log format as shown in Fig. 5. Using a log-log display, frequency content can conveniently be observed.

Figures 6, 7, and 8 are a similar set of plots but with the compressor operating. The major response frequency is about 8 Hz, which relates to the compressor rotation; a smaller contribution occurs at twice this frequency and may be related to the valve operating mechanism. Amplitude contribution as a function of frequency, obtained by integration of the power spectral density curves of Fig. 6, are presented in Fig. 7. Major amplitude response is at the compressor rotation frequency except at the 135 ft measurement location where several other frequencies are observed. The additional frequencies may be caused by the proximity of location 135 ft to another building having its own characteristic excitation sources.

Figures 9, 10, and 11 are acceleration response plots of the background noise response with the compressor not operating. The plots are similar to Figs. 3, 4, and 5 except that the higher frequencies are accentuated due to the fact that the acceleration is equal to the frequency squared times the displacement. This results in the apparent amplitude increase at higher frequencies. Acceleration response resulting from compressor

operation is shown in Figs. 12, 13, and 14, where the f^2 response relationship can clearly be seen.

RMS displacements are plotted in Fig. 15. The results clearly illustrate the importance of providing vibration isolation of reciprocating machinery. In this case the compressor was mounted on a separate concrete pad with expansion joint material between the pad and building floor. The displacement signal as measured on the building floor was attenuated by 81 percent.

The transmissibility from the building floor to the ground outside the building is relatively high, the floor signal being attenuated by only 25 percent. Attenuation in the ground due to distance from the building is 75 percent at a distance of 100 feet.

Since the displacement and acceleration measurements were taken at slightly different times, the response may vary somewhat due to external excitation forces which may be time variant.

Using a measurement method similar to that used in this study, with a known force input to the soil, transfer functions can be obtained for evaluating the response coupling between various machinery, such as compressors and pumps, housed in auxiliary building and sensitive areas of the beam lines. The availability of multiple accelerometer channels, together with the application of correlation techniques, will allow for the determination of various wave speeds as well as the attenuation characteristics of the ground.

Table 1. RMS Displacement, (5 Hz - 100 Hz)

Location	Ambient Noise	Compressor On
Pad	2.27×10^{-6} in. (0.0577 μm)	1.09×10^{-4} in. (2.77 μm)
Floor	1.49×10^{-6} in. (0.0378 μm)	2.11×10^{-5} in. (0.536 μm)
5'	1.51×10^{-6} in. (0.0384 μm)	1.37×10^{-5} in. (0.348 μm)
50'	1.44×10^{-6} in. (0.0366 μm)	5.37×10^{-6} in. (0.136 μm)
93'	1.90×10^{-6} in. (0.0483 μm)	3.92×10^{-6} in. (0.0996 μm)
135'	-	4.63×10^{-6} in. (0.118 μm)

Table 2. RMS Acceleration (\approx 3 Hz - 100 Hz), g's

Location	Ambient Noise	Compressor On
Pad	2.06×10^{-4}	3.82×10^{-3}
Floor	4.18×10^{-4}	2.48×10^{-4}
5'	2.33×10^{-4}	3.21×10^{-4}
50'	-	-
93'	1.47×10^{-4}	-
135'	-	-

ROAD

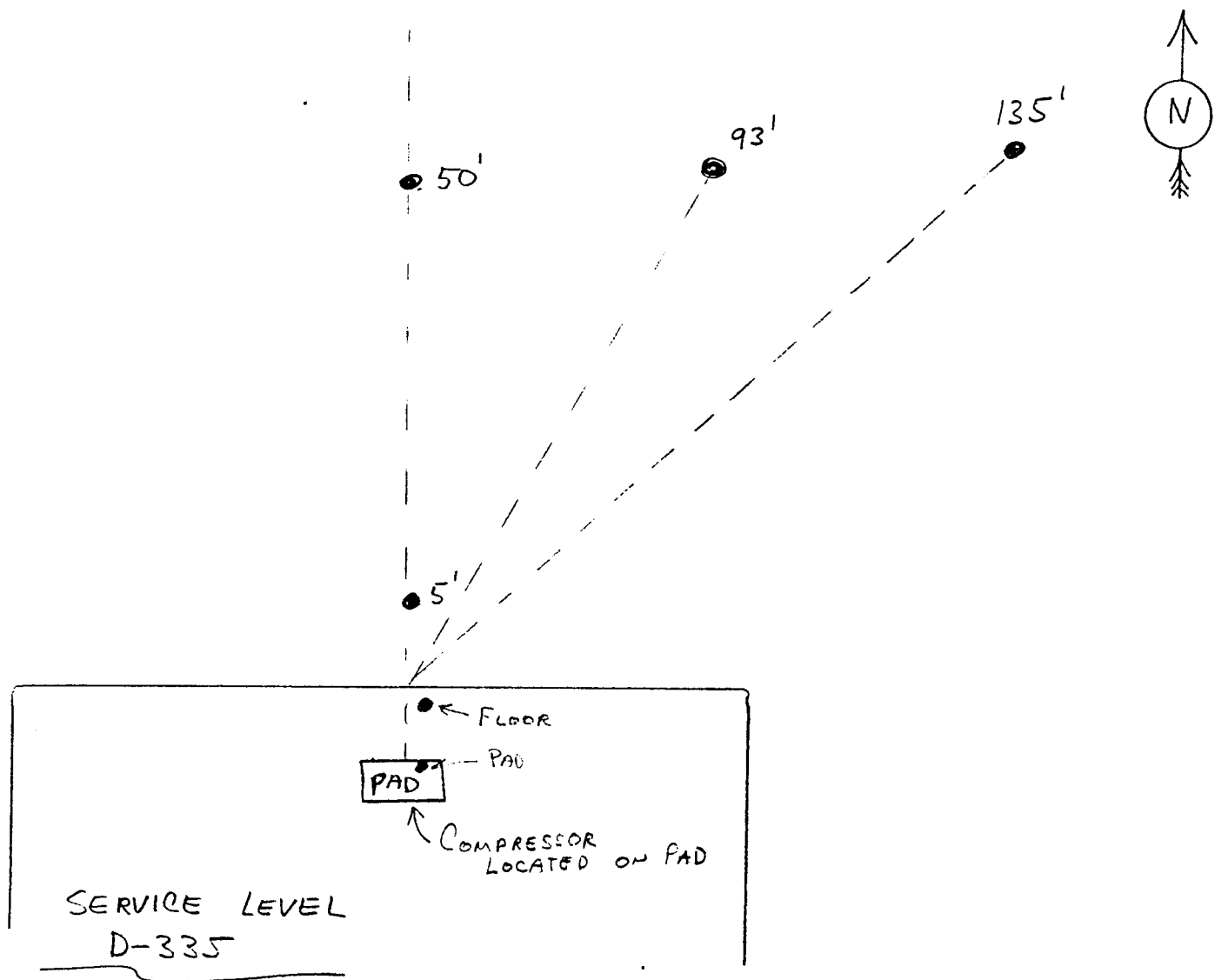
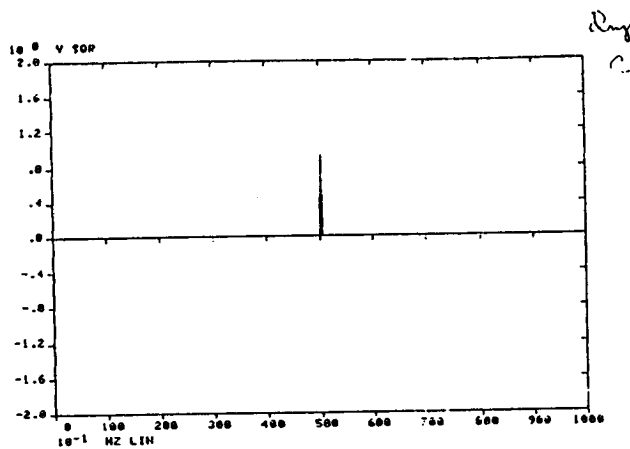
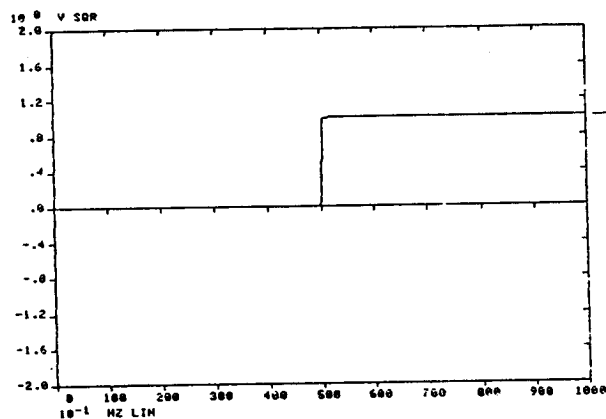


Fig. 1. Measurement Locations



50Hz SINEWAVE
@ 1.01V_{RMS} INPUT



← MS Volts Out

$$\frac{W_0 511}{SF (511)} \cdot \frac{-3}{1017} \cdot \frac{12}{15} \cdot \frac{15}{0} \sqrt{2} = 1.008 V_{RMS} \quad \underline{\text{OUTPUT VOLTAGE}}$$

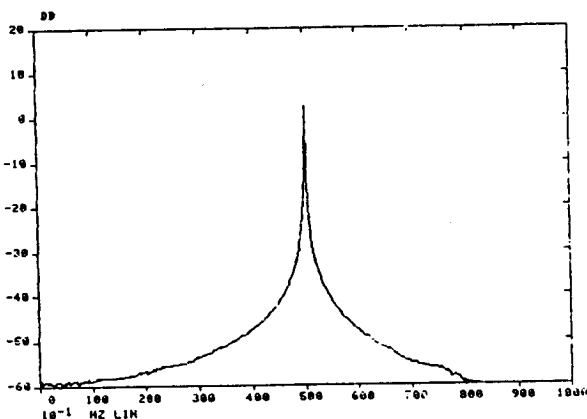
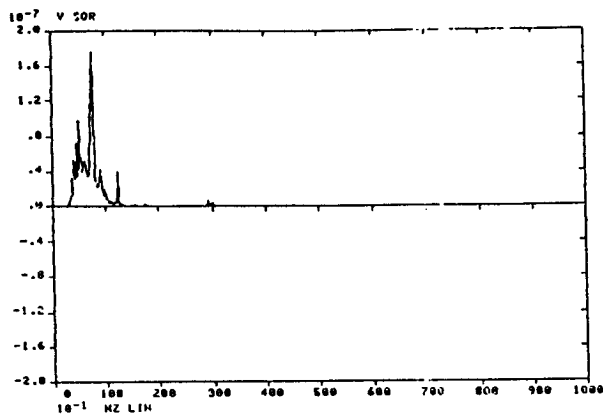
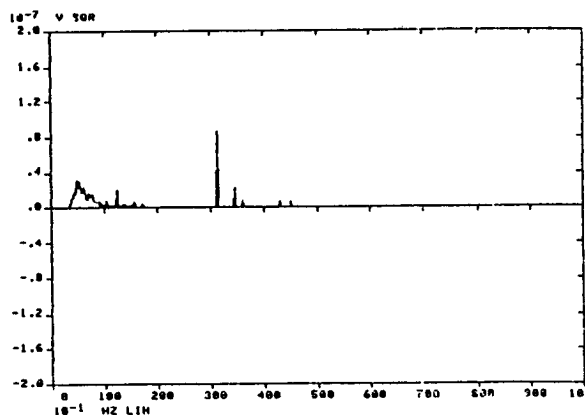


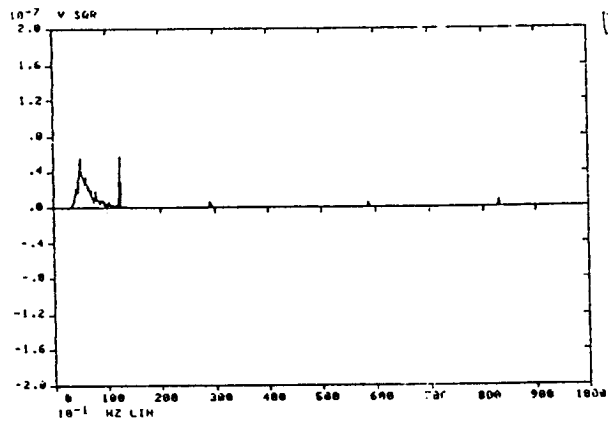
Fig. 2. Calibration Verification of 5451C FFT



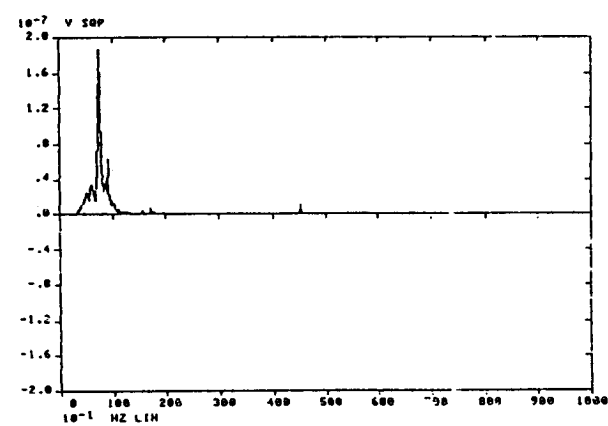
DISP
PAV
COFF



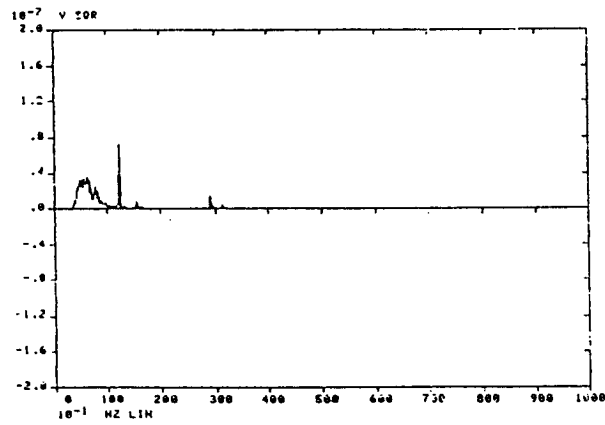
DISP
50'
COFF



DISP
FLOOR
COFF



DISP
93'
COFF



DISP
5'
COFF

Fig. 3. Displacement PSD - Ambient Noise Level
(Compressor Off)

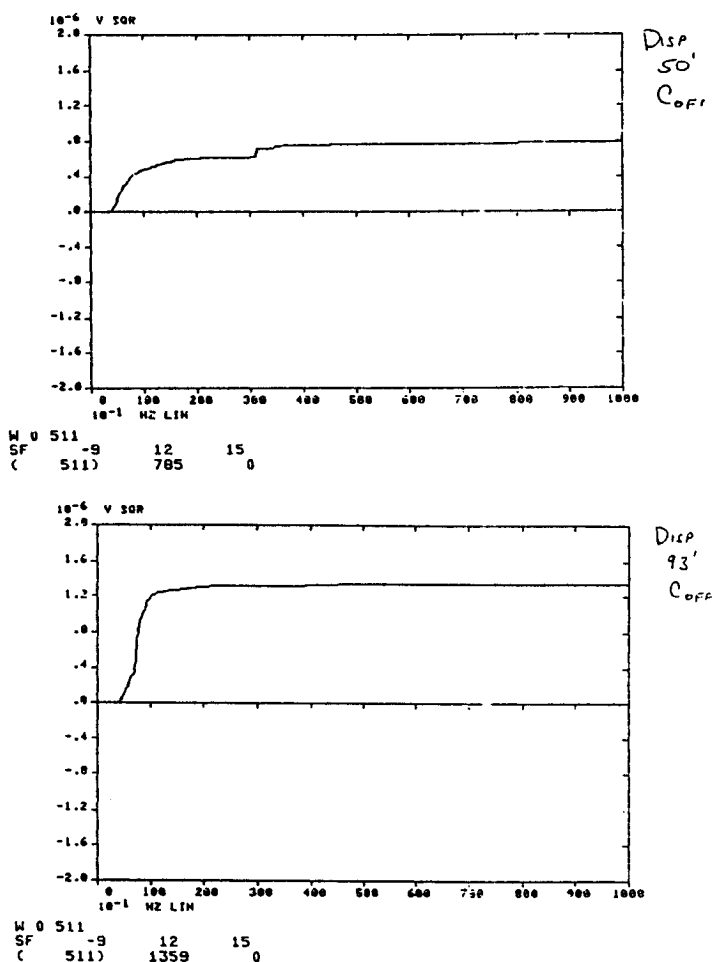
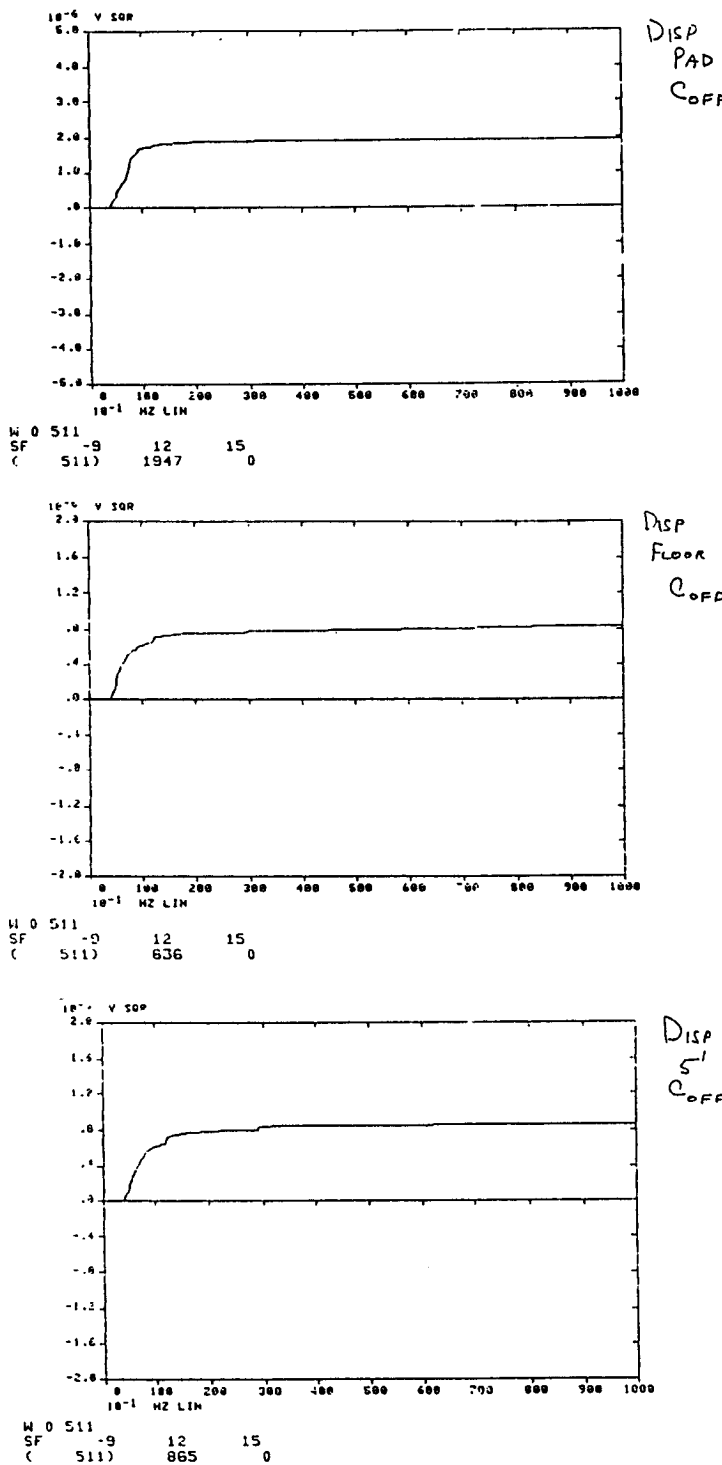


Fig. 4. Cumulative Contribution to Mean-Square Displacement - Ambient Noise Level (Compressor Off)

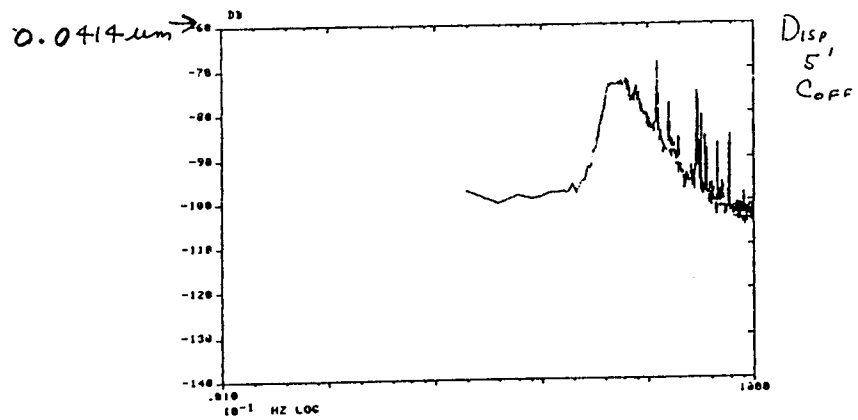
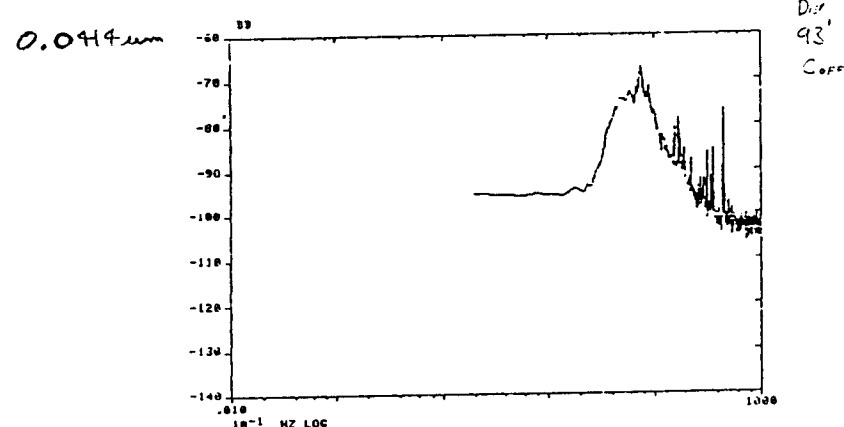
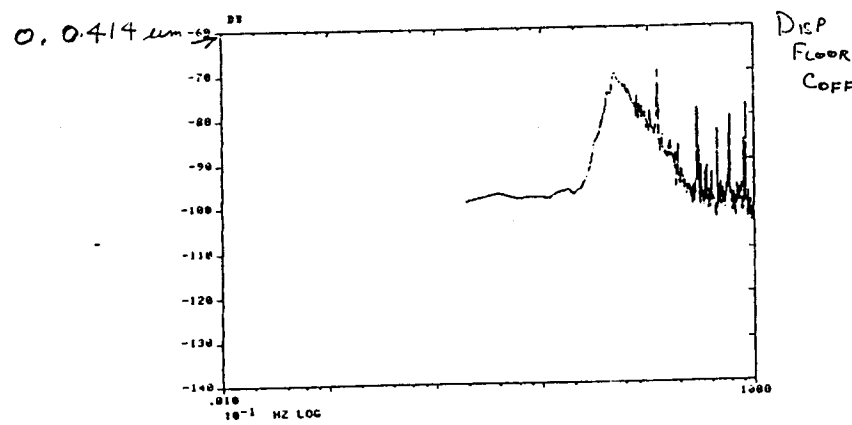
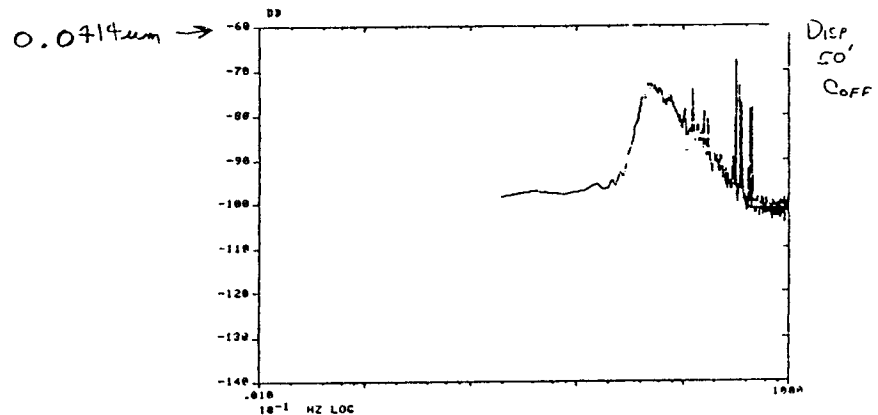
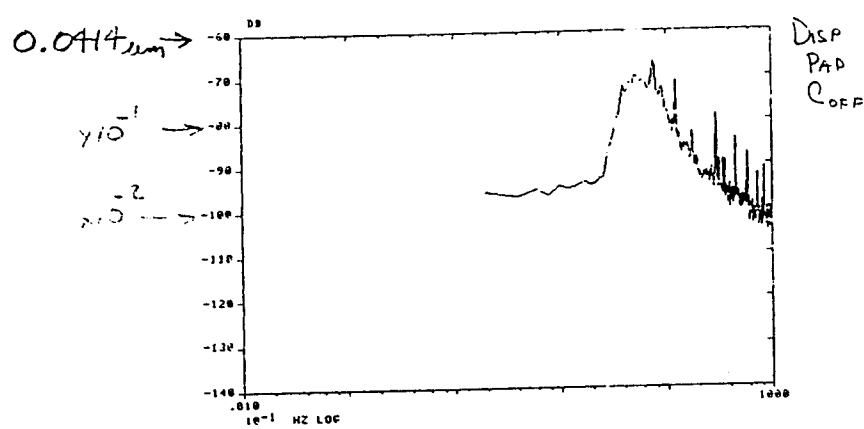


Fig. 5. Frequency Distribution of RMS Displacement - Ambient Noise Level (Compressor Off)

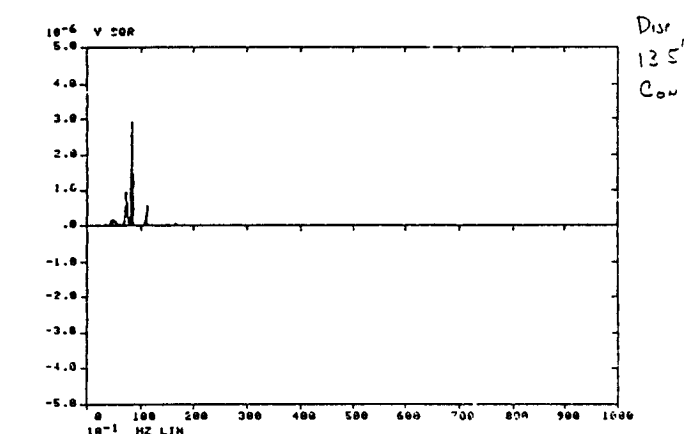
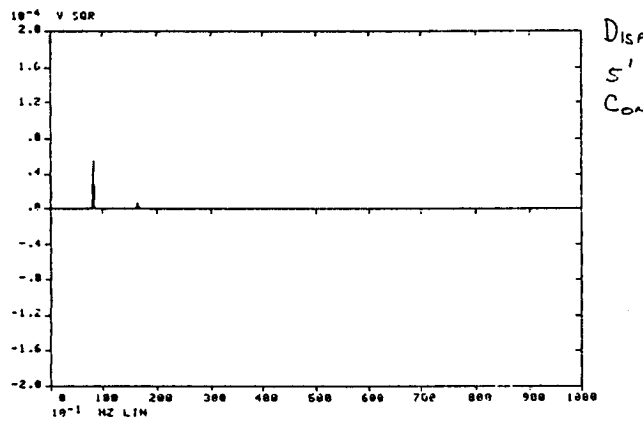
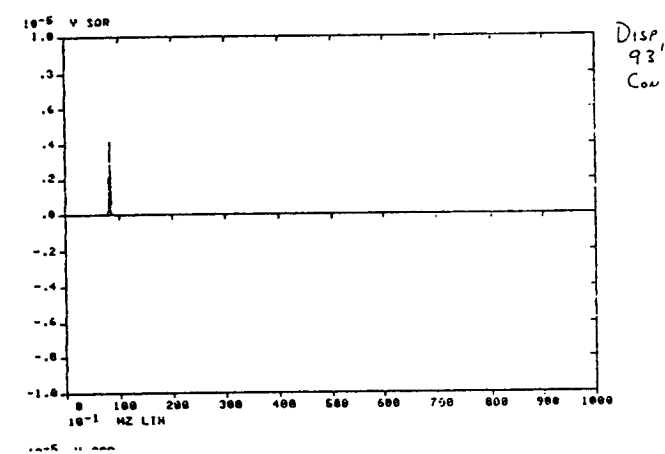
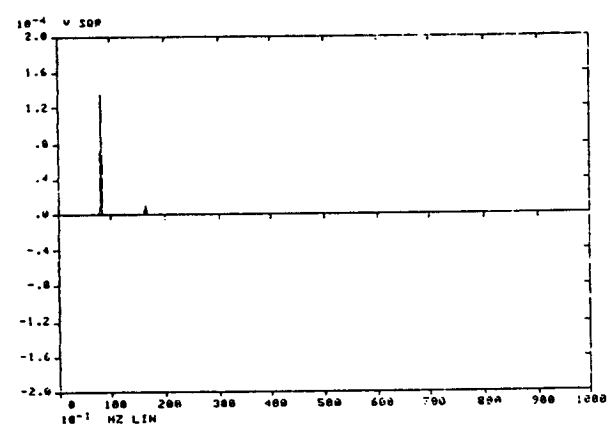
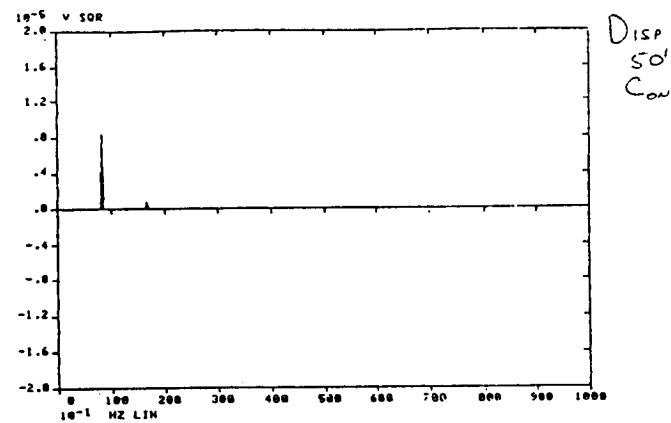
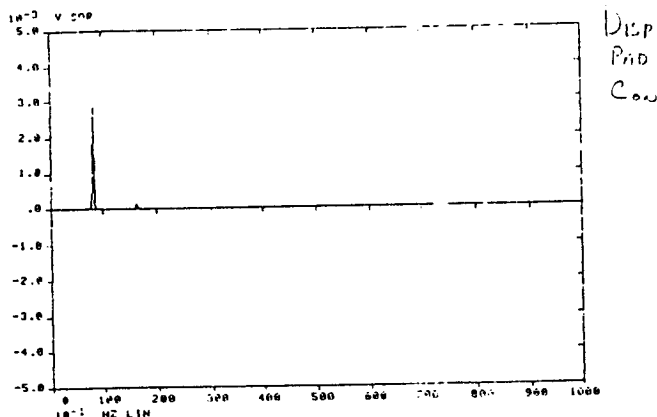
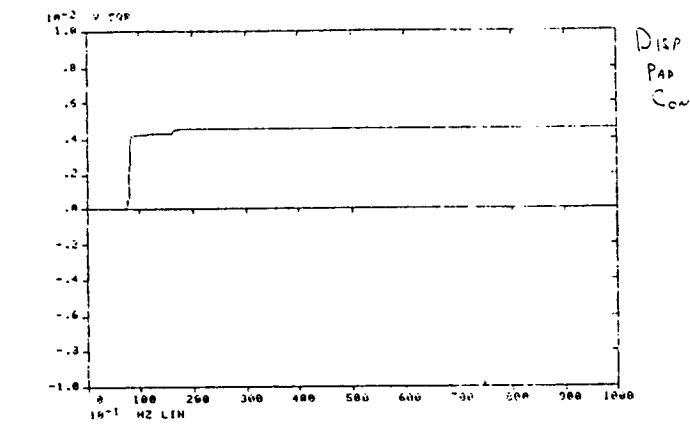
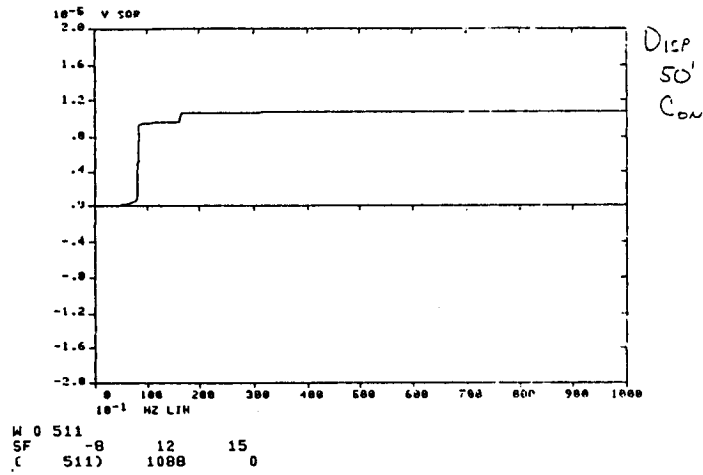


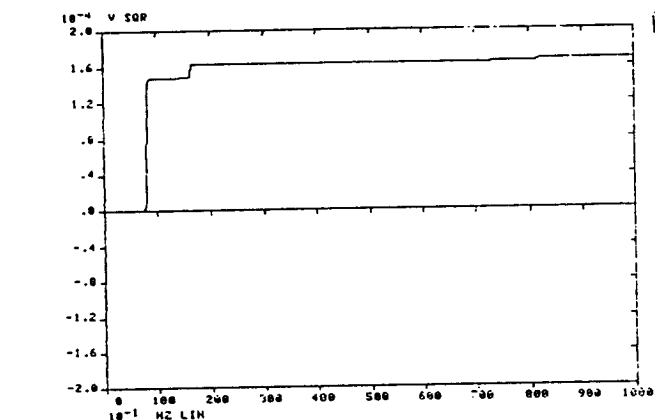
Fig. 6. Displacement PSDs at Measurement Locations (Compressor Operating)



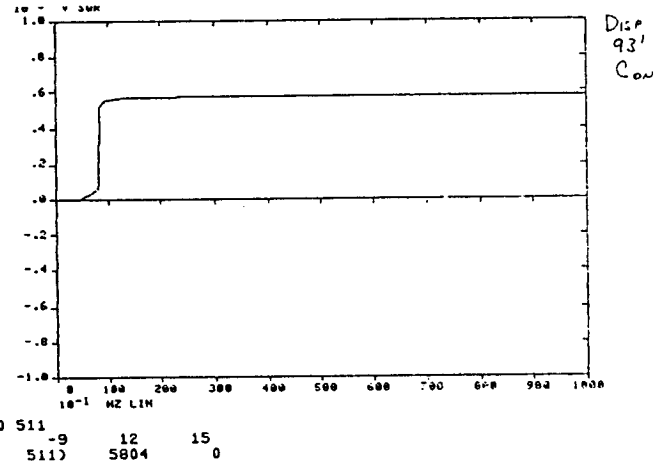
W 0 511
SF -6 12 15
(511) 4518 0



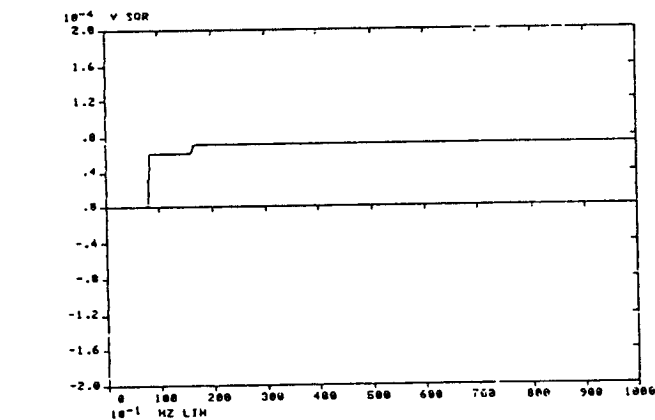
W 0 511
SF -8 12 15
(511) 1088 0



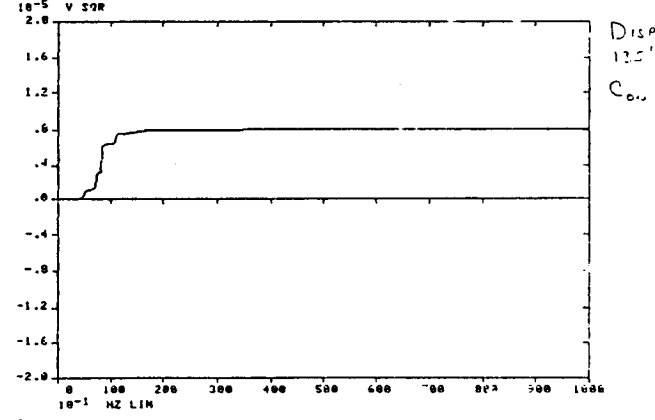
W 0 511
SF -7 12 15
(511) 1672 0



W 0 511
SF -9 12 15
(511) 5804 0



W 0 511
SF -8 12 15
(511) 7171 0



W 0 511
SF -8 12 15
(511) 809 0

Fig. 7. Cumulative Contribution to Mean-Square Displacements at Measurement Locations (Compressor Operating)

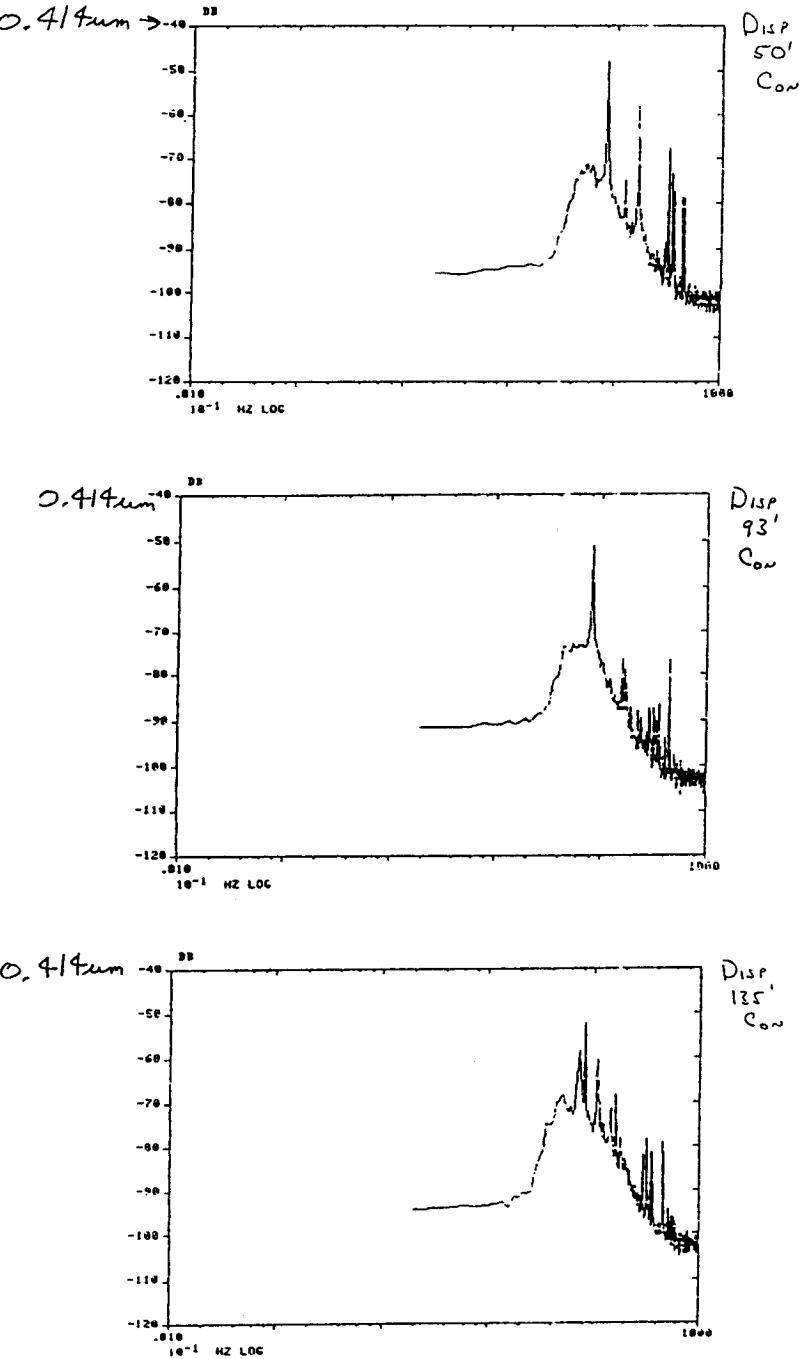
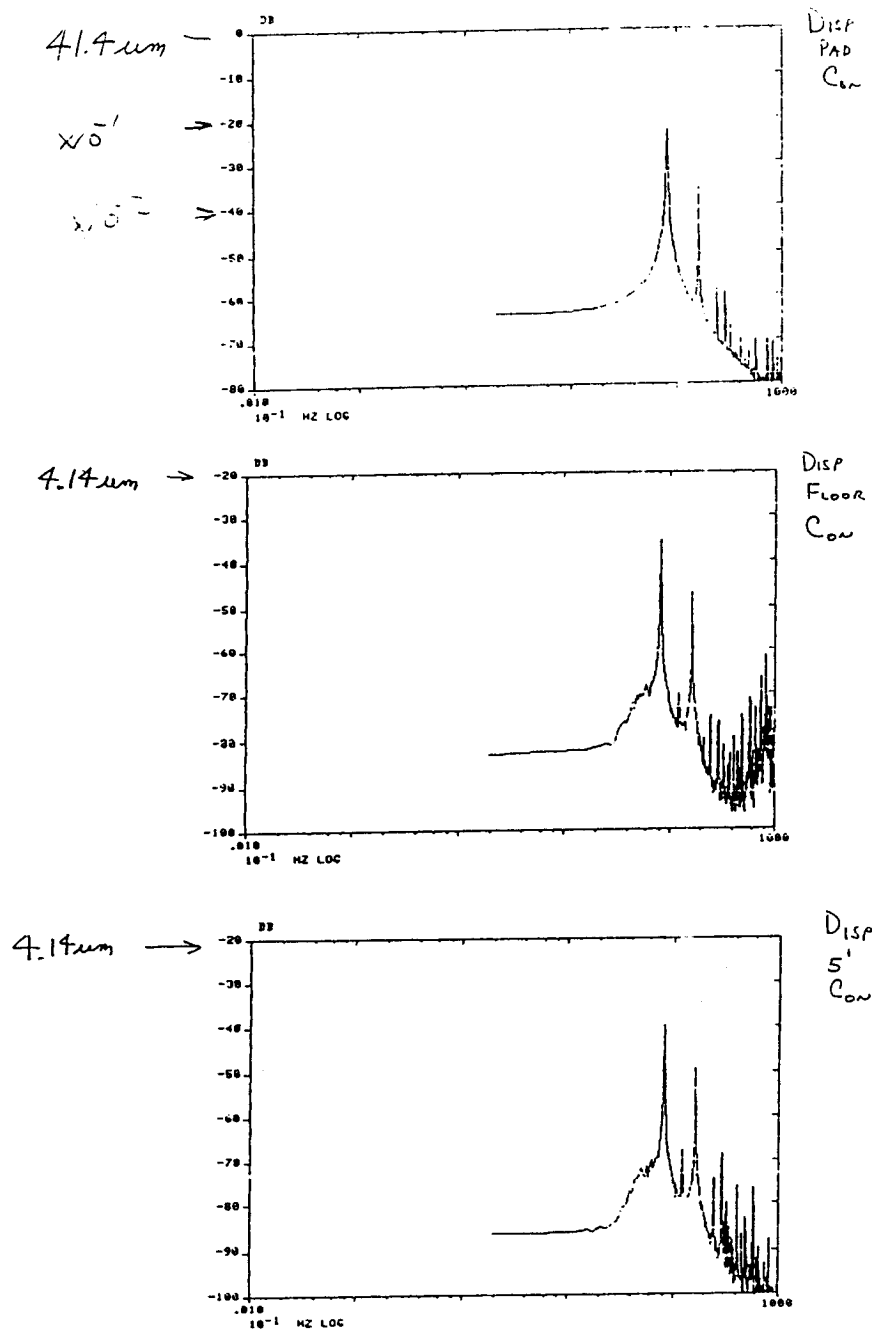


Fig. 8. Frequency Distribution of RMS Displacement at Measurement Locations
(Compressor Operating)

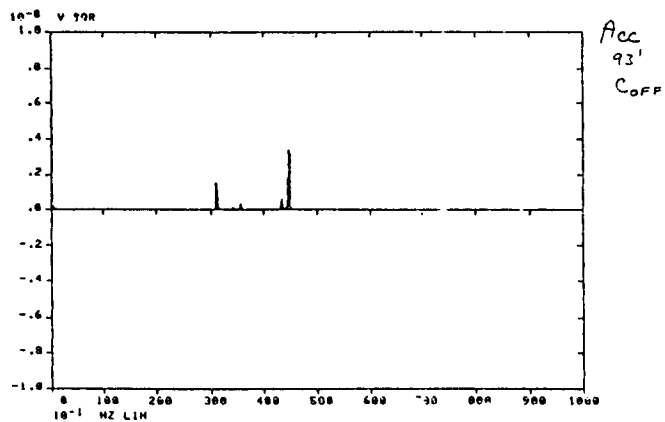
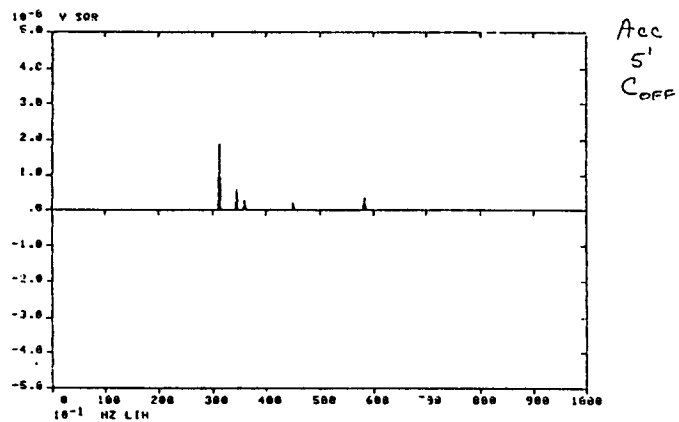
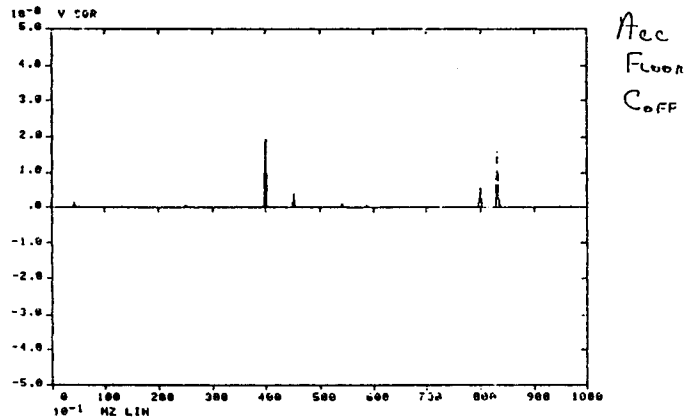
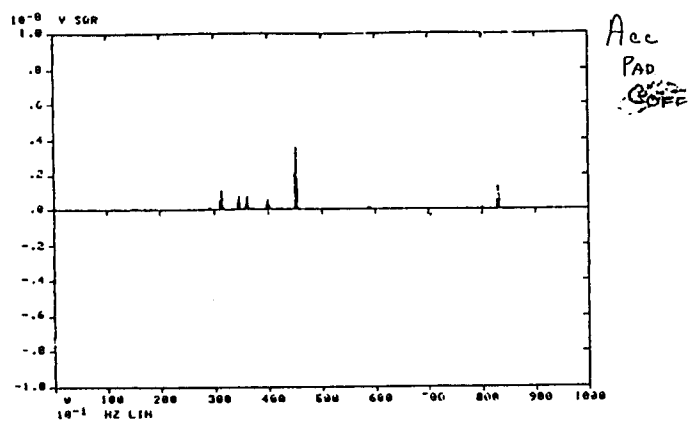


Fig. 9. Acceleration PSDs - Ambient Noise Level (Compressor Off)

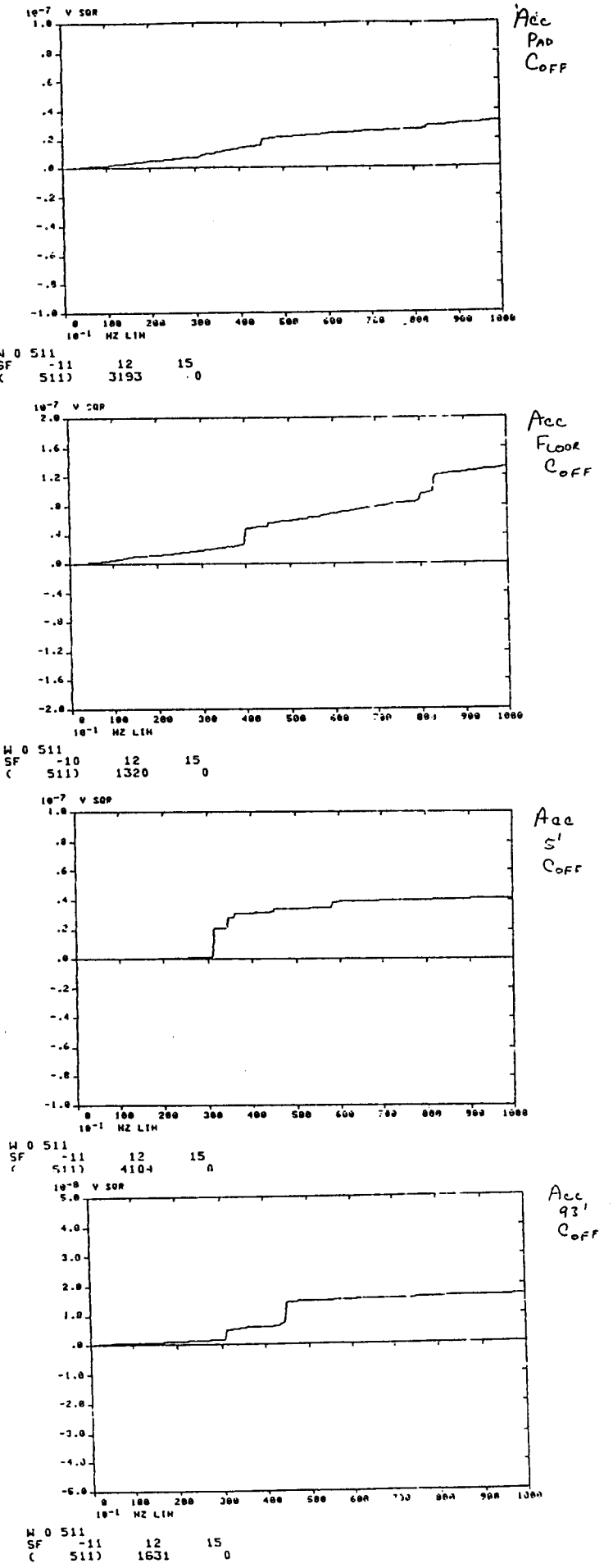


Fig. 10. Cumulative Contribution to Mean-Square Acceleration - Ambient Noise Level (Compressor Off)

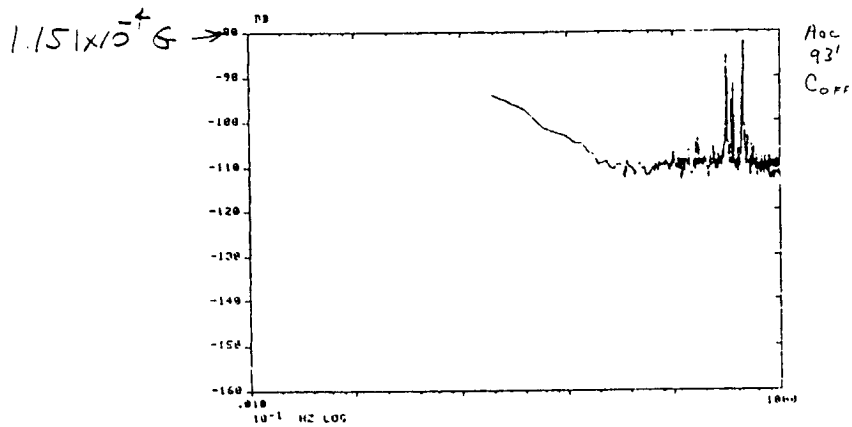
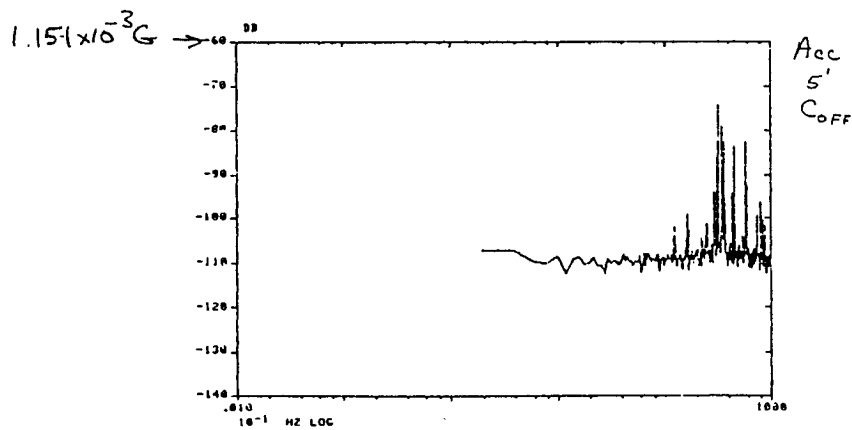
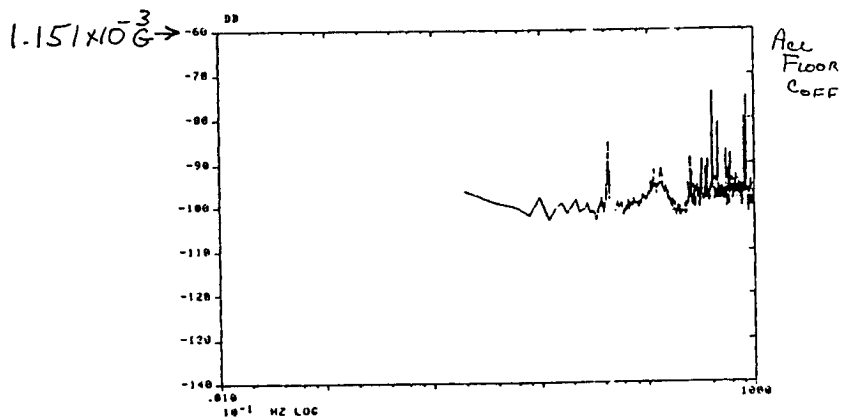
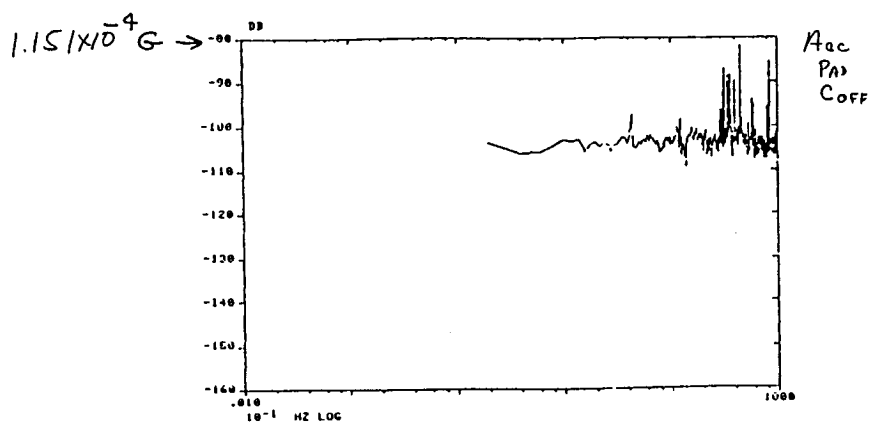


Fig. 11. Frequency Distribution of RMS Acceleration - Ambient Noise Level (Compressor Off)

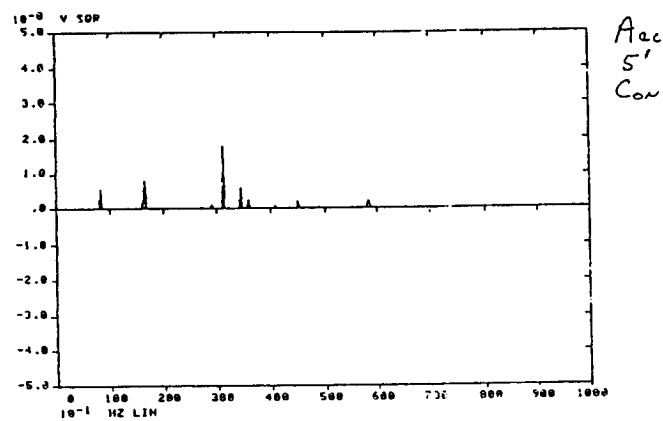
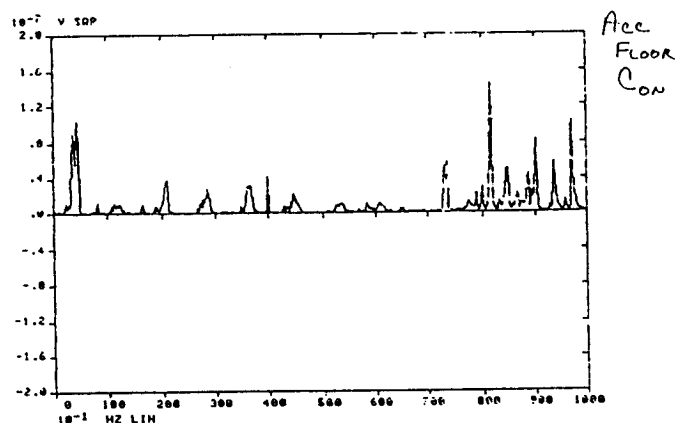
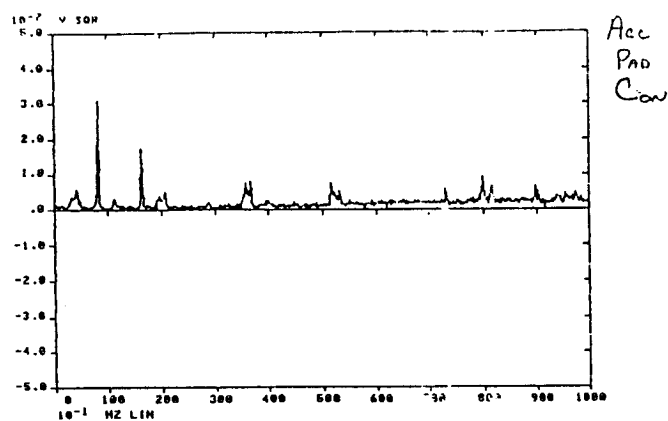


Fig. 12. Acceleration PSDs at Measurement Locations
(Compressor Operating)

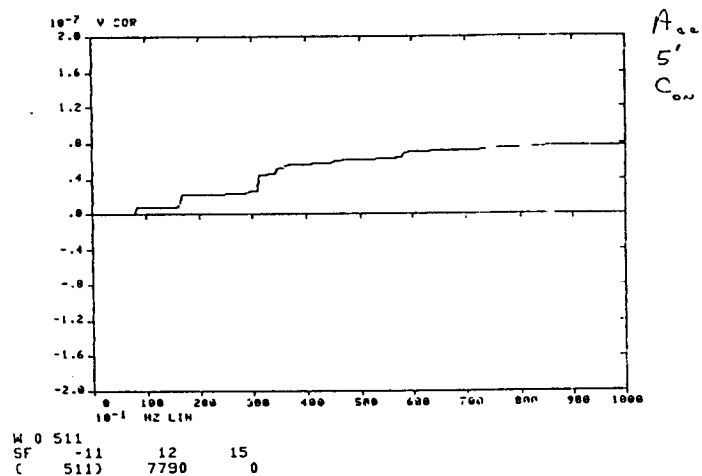
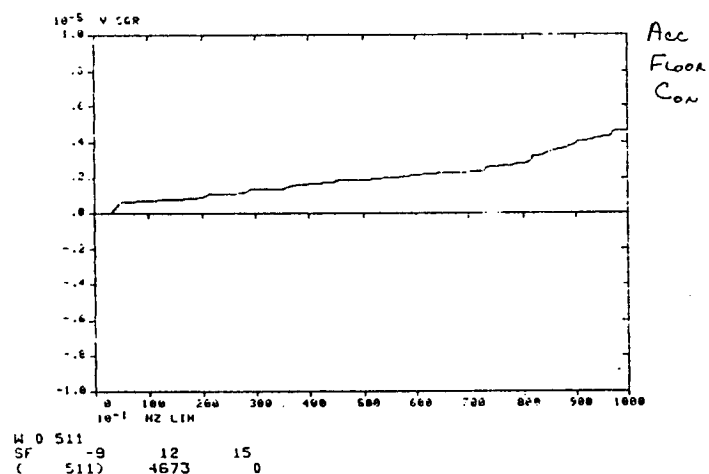
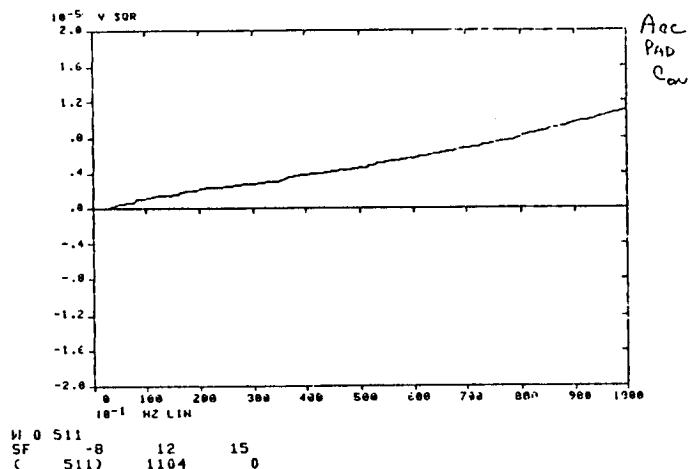


Fig. 13. Cumulative Contribution to Mean-Square Acceleration at Measurement Locations (Compressor Operating)

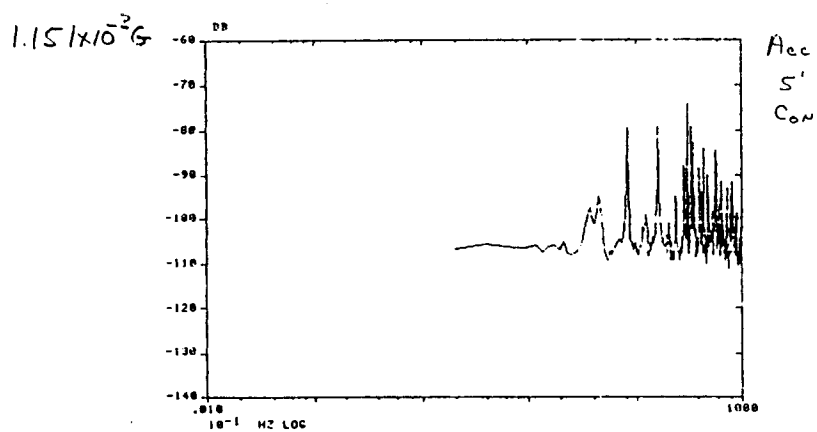
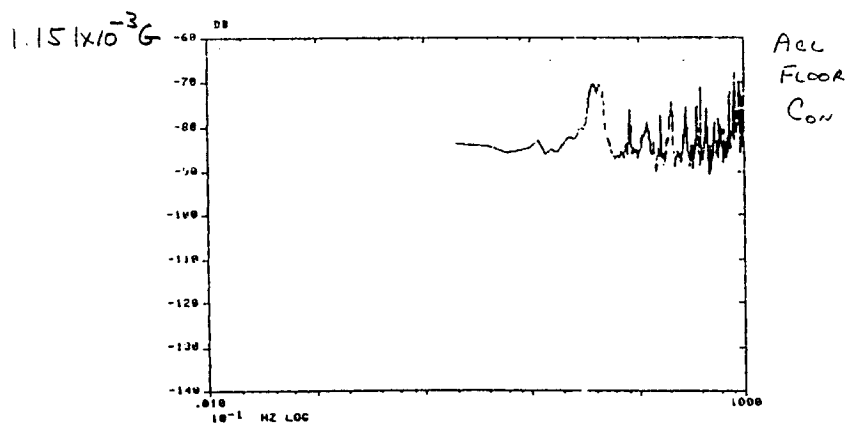
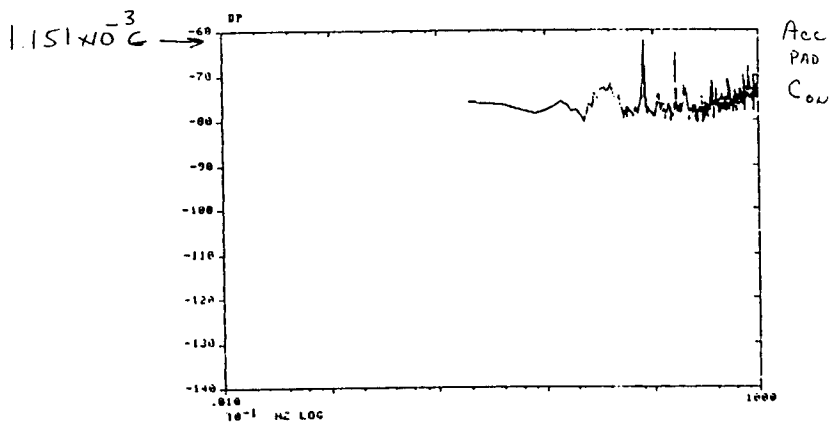


Fig. 14. Frequency Distribution of RMS Acceleration at Measurement Locations (Compressor Operating)

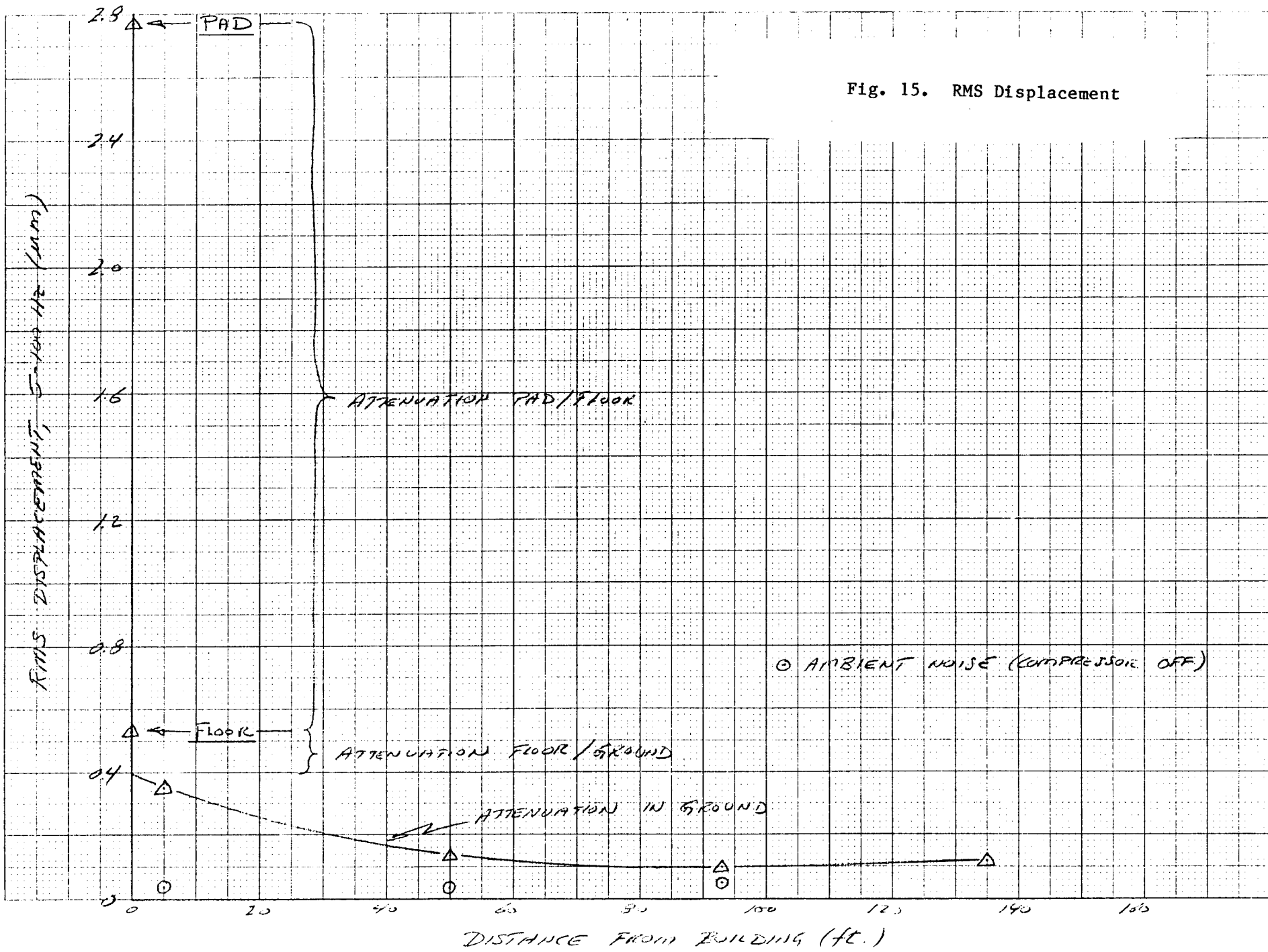


Fig. 15. RMS Displacement